



## Short Communication

CO<sub>2</sub> hydrogenation to methanol over Cu/ZnO/ZrO<sub>2</sub> catalysts prepared via a route of solid-state reactionXiaoming Guo<sup>a,b</sup>, Dongsen Mao<sup>b,\*</sup>, Guanzhong Lu<sup>a,b,\*</sup>, Song Wang<sup>b</sup>, Guisheng Wu<sup>b</sup><sup>a</sup> Research Institute of Industrial Catalysis, East China University of Science and Technology, Shanghai 200237, PR China<sup>b</sup> Research Institute of Applied Catalysis, School of Chemical and Environmental Engineering, Shanghai Institute of Technology, Shanghai 200235, PR China

## ARTICLE INFO

## Article history:

Received 19 January 2011

Received in revised form 21 March 2011

Accepted 22 March 2011

Available online 27 March 2011

## Keywords:

Cu/ZnO/ZrO<sub>2</sub> catalyst

Solid-state reaction

CO<sub>2</sub> hydrogenation

Methanol

## ABSTRACT

Cu/ZnO/ZrO<sub>2</sub> catalysts were prepared by a route of solid-state reaction and tested for the synthesis of methanol from CO<sub>2</sub> hydrogenation. The effects of calcination temperature on the physicochemical properties of as-prepared catalysts were investigated by N<sub>2</sub> adsorption, XRD, TEM, N<sub>2</sub>O titration and H<sub>2</sub>-TPR techniques. The results show that the dispersion of copper species decreases with the increase in calcination temperature. Meanwhile, the phase transformation of zirconia from tetragonal to monoclinic was observed. The highest activity was achieved over the catalyst calcined at 400 °C. This method is a promising alternative for the preparation of highly efficient Cu/ZnO/ZrO<sub>2</sub> catalysts.

© 2011 Elsevier B.V. All rights reserved.

## 1. Introduction

The hydrogenation of CO<sub>2</sub> to methanol, which is an important feedstock for the organic chemical industry and a potential alternative to fossil fuels, has received considerable attention from the viewpoint of environmental protection and effective utilization of carbon resources [1]. Catalysts based on Cu, especially Cu/ZnO/ZrO<sub>2</sub>, are highly effective for the synthesis of methanol from CO<sub>2</sub> hydrogenation and have been investigated extensively [2–6]. These Cu-based catalysts are usually prepared by co-precipitation from aqueous solutions [7,8]. However, precise pH control and long aging time of the suspension are required for this method. Furthermore, tedious washing is indispensable since residual alkaline metals have a negative effect on the catalytic activity [5]. Although some other methods such as hydrothermal [9], sol-gel [10,11] and reverse microemulsion techniques [12], have also been developed to prepare Cu-based catalysts, most of them suffer from complexity and time-consuming procedures and/or requirement of expensive starting materials [13]. Therefore, the development of novel and effective techniques for preparing Cu-based catalysts is imperative and significant. Recently, we reported the preparation of highly effective Cu/ZnO/ZrO<sub>2</sub> catalysts by urea-nitrate and glycine-nitrate combustion method [14,15]. On the other hand, Xin et al. [16,17] developed a novel solid-state synthesis approach, in which solid state metathesis reactions occur between hydrated transition metal salts and organic ligands (or hydroxides), to yield metal complexes, metal clusters or

oxides with uniform sizes and shapes. This method has attracted extensive research interest because it is a simple, rapid, solvent-free, and energy-saving process. With this method, Cu/ZnO catalysts were recently prepared by Wang et al. for steam reforming of methanol, and special attention was paid to the effects of the grinding time on the structural properties and catalytic behavior [13].

In this paper, Cu/ZnO/ZrO<sub>2</sub> catalysts were prepared via a route of solid-state chemical reaction between hydrated metal salts and citric acid ligand. The physicochemical properties of as-prepared Cu/ZnO/ZrO<sub>2</sub> were characterized by XRD, BET, TEM, reactive N<sub>2</sub>O adsorption and TPR techniques, and the catalytic activity for methanol synthesis from CO<sub>2</sub> hydrogenation was evaluated. Since the calcination process is a key step in the route of solid-state reaction for the preparation of copper catalyst, this study emphasizes the effects of calcination temperature on the properties of the derived Cu/ZnO/ZrO<sub>2</sub> catalysts. Meanwhile, the relationship between the physicochemical properties and the catalytic performance was discussed.

## 2. Experimental

## 2.1. Catalyst preparation

Firstly, analytical grade Cu(NO<sub>3</sub>)<sub>2</sub>·3H<sub>2</sub>O, Zn(NO<sub>3</sub>)<sub>2</sub>·6H<sub>2</sub>O and Zr(NO<sub>3</sub>)<sub>4</sub>·5H<sub>2</sub>O were blended to form a homogenized premix, in which the molar ratio of Cu<sup>2+</sup>, Zn<sup>2+</sup> and Zr<sup>4+</sup> meets the formula of (CuO)<sub>0.5</sub>(ZnO)<sub>0.2</sub>(ZrO<sub>2</sub>)<sub>0.3</sub> (CZZ). Then citric acid (C<sub>6</sub>H<sub>8</sub>O<sub>7</sub>·H<sub>2</sub>O), a ligand for metal cations of Cu<sup>2+</sup>, Zn<sup>2+</sup> and Zr<sup>4+</sup>, was added to the premix and ground in an agate mortar at room temperature. The molar ratio of C<sub>6</sub>H<sub>8</sub>O<sub>7</sub>·H<sub>2</sub>O to the metal ions was 1.3:1. After being ground for 30 min, all the reactants transferred to a uniform, viscous and muddy

\* Corresponding authors. Tel./fax: +86 21 6494 1386.

E-mail addresses: [dsmo1106@yahoo.com.cn](mailto:dsmo1106@yahoo.com.cn) (D. Mao), [gzhlu@ecust.edu.cn](mailto:gzhlu@ecust.edu.cn) (G. Lu).

precursor for the CZZ catalysts. Thereafter the precursor was dried at 110 °C for 6 h and further calcined in air at a certain temperature (400–800 °C) for 4 h. The resulted CZZ powders were termed as CZZ-400, CZZ-500, CZZ-600, CZZ-700 and CZZ-800.

## 2.2. Catalyst characterization

The thermal gravimetric and differential thermal analysis (TG-DTA) profiles of the CZZ precursor were recorded on a thermal analyzer (SDT Q-600, Thermal Analysis Instruments) at a heating rate of 10 °C/min under an air stream of 100 ml/min.

Cu contents of the calcined catalysts were determined by atomic absorption spectroscopy (AAS) on acid-digested samples, using a SpectrAA-220 Atomic absorption spectrometer (VARIAN).

X-ray diffraction (XRD) analysis of sample was performed using a PANalytical X'Pert diffractometer operating with Ni  $\beta$ -filtered Cu  $K_{\alpha}$  radiation at 40 kV and 40 mA. Two theta angles ranged from 20 to 70° with a speed of 6° per minute. The crystallite size of CuO ( $d_{\text{CuO}}$ ) was calculated from the XRD spectra by using the Scherrer equation.

Transmission electron microscopy (TEM) experiment was conducted on a JEOL 2010 microscope operated at 200 kV. The samples were suspended in ethanol and supported onto a holey carbon film on a Cu grid.

The BET surface areas of the samples were determined by N<sub>2</sub> adsorption isotherms, using a Micromeritics ASAP2020 M+C adsorption apparatus. The samples were evacuated at 200 °C for 3 h prior to N<sub>2</sub> dosage.

The surface compositions of the samples were investigated by X-ray photoelectron spectroscopy (XPS, Perkin-Elmer PHI 5000C ESCA) using Al  $K_{\alpha}$  radiation. All the binding energy values were calibrated by using C 1s = 284.6 eV as a reference.

The metallic copper surface areas ( $S_{\text{Cu}}$ ) in the reduced catalysts were determined by the N<sub>2</sub>O reactive frontal chromatography technique at 60 °C assuming a Cu:N<sub>2</sub>O = 2 titration stoichiometry and a surface atomic density of  $1.46 \times 10^{19}$  copper atoms per m<sup>2</sup>, respectively [15]. The copper dispersion ( $D_{\text{Cu}}$ ), defined as the amount of exposed copper in relation to the total amount of copper atoms, was calculated for the reduced catalysts.

Temperature-programmed reduction (TPR) measurements were performed in a continuous-flow apparatus fed with a 10% H<sub>2</sub>/N<sub>2</sub> mixture and heated at a rate of 5 °C/min. A ca. 30-mg catalyst sample was used, with H<sub>2</sub> consumption monitored by a TCD.

## 2.3. Catalyst testing

Activity and selectivity measurements for CO<sub>2</sub> hydrogenation were carried out in a continuous-flow, fixed-bed reactor. Prior to the catalytic measurements, the fresh catalyst was reduced in a stream of 10% H<sub>2</sub>/N<sub>2</sub> at 300 °C for 3 h under atmospheric pressure. Then, the reactor was cooled to a given temperature and the reactant gas (CO<sub>2</sub>: H<sub>2</sub> = 1:3, molar ratio) flow was introduced, raising the pressure to

3.0 MPa. All post-reactor lines and valves were heated to 140 °C to prevent the condensation of the products. Effluent products were analyzed on-line with a gas chromatograph (6820, Agilent). Methanol was determined with a Porapak Q column, a FID and other gaseous products were determined with a Carbosieve column, a TCD. Conversion and selectivity values were calculated by mass-balance method and the steady-state values are quoted as the average of four different analyses.

## 3. Results and discussion

### 3.1. The formation of CZZ catalysts

There are two steps involved in the formation of CZZ catalysts with the route of solid-state reaction. First, complexes of metal-citrate were prepared by the solid-state reaction between hydrated metal salt and citric acid. Then, CuO–ZnO–ZrO<sub>2</sub> was obtained by decomposition of the Cu–Zn–Zr citrate precursor. The TG-DTA profiles (not shown) of the citrate precursor suggest that the precursor cannot be decomposed completely at the temperature less than 400 °C. Accordingly, the minimum calcination temperature of 400 °C was chosen in the present paper.

The Cu contents of the catalysts, as determined by AAS, are given in Table 1. The values of Cu contents for all the samples are very close to the theoretical value (34.2 wt.%), indicating that the composition of CZZ catalysts prepared via the route of solid-state reaction can be precisely controlled.

### 3.2. Textural and structural properties

Fig. 1 shows the XRD patterns of the dried precursor for CZZ and the CZZ powders calcined at different temperatures. The dried precursor is primarily amorphous in structure for no diffraction peak can be observed. Weak and broad diffraction peaks of CuO phase (JCPDS 80–1268) appear at 2 $\theta$  of 35.6°, 38.8° as the powder is calcined at 400 °C. At the same time, a much broader and weaker diffraction peak at 2 $\theta$  of 30.2°, which is ascribed to the tetragonal zirconia (*t*-ZrO<sub>2</sub>, JCPDS 88–1007), appears and no diffraction peak of ZnO phase can be detected. These results indicate that a low crystallization degree of metal oxides was obtained in the CZZ-400 sample. With the increase in calcination temperature, the diffraction peaks of CuO and *t*-ZrO<sub>2</sub> become stronger and sharper simultaneously, indicating a continuous increase in the crystallization degree of CuO and *t*-ZrO<sub>2</sub>. As the calcination temperature is raised to 600 °C, the peaks of the monoclinic ZrO<sub>2</sub> (*m*-ZrO<sub>2</sub>, JCPDS 83–0940) phase and the ZnO (JCPDS 36–1451) phase begin to appear. When the calcination temperature is higher than 700 °C, the intensity of *t*-ZrO<sub>2</sub> peak decreases whereas that of *m*-ZrO<sub>2</sub> peak increases. The phenomenon demonstrates the partial transformation of the ZrO<sub>2</sub> phase from tetragonal to monoclinic with the rise of calcination temperature [18]. For CZZ-800 sample, the characteristic peak of *t*-ZrO<sub>2</sub> vanishes, suggesting that *t*-

**Table 1**  
Physicochemical and catalytic properties of the Cu/ZnO/ZrO<sub>2</sub> catalysts calcined at different temperatures.

Catalyst	Average Cu content (wt.%) <sup>a</sup>	Surface Cu content (wt.%) <sup>b</sup>	$d_{\text{CuO}}$ (nm)	$S_{\text{BET}}$ (m <sup>2</sup> /g)	$S_{\text{Cu}}$ (m <sup>2</sup> /g)	$D_{\text{Cu}}$ <sup>c</sup> (%)	CO <sub>2</sub> conversion (%)	CH <sub>3</sub> OH selectivity (%)	CH <sub>3</sub> OH yield (%)
CZZ-400	33.1%	26.9	8.0	58.6	12.6	5.7	15.7	58.0	9.1
CZZ-500	33.2%	–	11.3	34.7	7.8	3.5	14.5	57.7	8.4
CZZ-600	33.4%	23.5	15.1	11.7	3.9	1.8	14.0	56.0	7.8
CZZ-700	33.8%	–	22.1	5.1	1.7	0.8	10.2	56.2	5.7
CZZ-800	33.7%	18.4	30.6	2.3	0.8	0.4	5.1	63.3	3.2

Reaction conditions: T = 240 °C, CO<sub>2</sub>:H<sub>2</sub> = 1:3, P = 3.0 MPa, GHSV = 3600 h<sup>-1</sup>.

Experimental errors of the CO<sub>2</sub> conversion and CH<sub>3</sub>OH selectivity are within  $\pm 3\%$ .

<sup>a</sup> Determined by AAS method.

<sup>b</sup> Determined by XPS method.

<sup>c</sup>  $D_{\text{Cu}}$  = exposed copper atoms/total copper atoms.

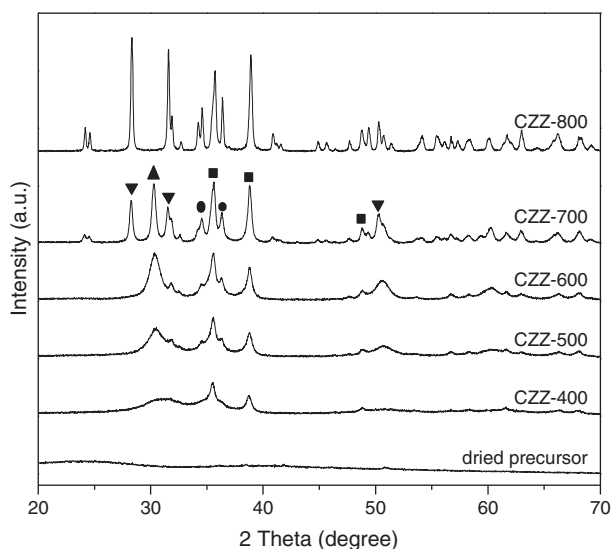


**Fig. 1.** XRD patterns of the dried precursor and the CZZ powders calcined at different temperatures. (■) CuO; (●) ZnO; (▲) ZrO<sub>2</sub> (tetragonal); (▼) ZrO<sub>2</sub> (monoclinic).

ZrO<sub>2</sub> transformed to *m*-ZrO<sub>2</sub> completely. Furthermore, the mean crystallite size of CuO, which is estimated using the Scherrer equation, increases from 8.0 nm of CZZ-400 to 30.6 nm of CZZ-800, as shown in Table 1.

Fig. 2 shows the TEM images of the CZZ powders calcined under different temperatures. It can be seen that the particles of catalysts are nearly spherical geometry. The sample CZZ-400 exhibits uniform size distribution in the range of 4–6 nm and the grain sizes of sample CZZ-600 vary from 12 to 15 nm. For sample CZZ-800, a phenomenon of agglomeration can be observed and the grain size exceeds 30 nm. These results are in good agreement with the crystallite size calculated from XRD data.

It can be seen from Table 1 that the BET surface area decreases from 58.6 m<sup>2</sup>/g of CZZ-400 to 2.3 m<sup>2</sup>/g of CZZ-800. Meanwhile, the values of  $S_{Cu}$  and  $D_{Cu}$  decrease with the increase in calcination temperature and the variation trend is consistent with the result of XRD. The growth of crystal grain and/or the agglomeration of particle with the increase in calcination temperature are responsible for the change of  $S_{BET}$ ,  $S_{Cu}$  and  $D_{Cu}$ .

The surface Cu contents of three representative samples, as determined by XPS measurements, are presented in Table 1. It can be seen that the surface Cu contents of the CZZ catalysts are far lower than the average Cu content in the bulk catalyst (the second column in Table 1). The reason can be ascribed to enrichment of Zn and Zr on the surface of catalysts and similar results were reported by Słoczyński et al. [7]. Meanwhile, the surface Cu contents decrease drastically with the increase in calcination temperature, indicating that the effect of the enrichment of Zn and Zr over the surface of catalysts enhances with the increase in calcination temperature.

### 3.3. The reducibility of the catalysts

From Fig. 3, it can be seen that all the CZZ samples exhibit a broad band of H<sub>2</sub> consumption in the range of 175–275 °C. The shape of this band of H<sub>2</sub> consumption, which is asymmetric with a shoulder or a tail, is the result of a complex overlapping of several elemental reduction processes. Since ZnO and ZrO<sub>2</sub> are not reduced within the experimental regions [19,20], the reduction peaks are related to the reduction of different CuO species. To gain more insight into the TPR results, the broad bands are deconvoluted and two peaks, which are denoted as  $\alpha$  and  $\beta$  peaks, are obtained. The  $\alpha$  and  $\beta$  peaks are attributed to the reduction of small and large CuO particle, respectively [3,21]. The peak

positions and the relative contribution of  $\alpha$  peak to the TPR pattern are summarized in Table 2. With the calcination temperature increasing, the positions of  $\alpha$  peak and  $\beta$  peak shift to higher temperatures accompanied by a decrease in the fraction of  $\alpha$  peak. This indicates that the particle sizes of CuO increase from CZZ-400 to CZZ-800 because the higher the reduction temperature is, the larger the CuO particle will be [3]. Meanwhile, it suggests that the fractions of the small CuO particle in these catalysts decrease as the calcination temperature increases. These results are in good agreement with the results of XRD and N<sub>2</sub>O titration techniques. Furthermore, there is no notable difference of the integrated area of the TPR peak over the different samples, suggesting that the total hydrogen consumption is basically equal.

### 3.4. Catalytic performance

The catalytic activity and selectivity for CO<sub>2</sub> hydrogenation to methanol had been investigated over the as-prepared CZZ catalysts. Carbon monoxide and methanol are the only carbon-containing products under the used reaction conditions and trace of methane can be detected at high reaction temperatures. The effect of calcination temperature used during catalyst preparation on the catalytic

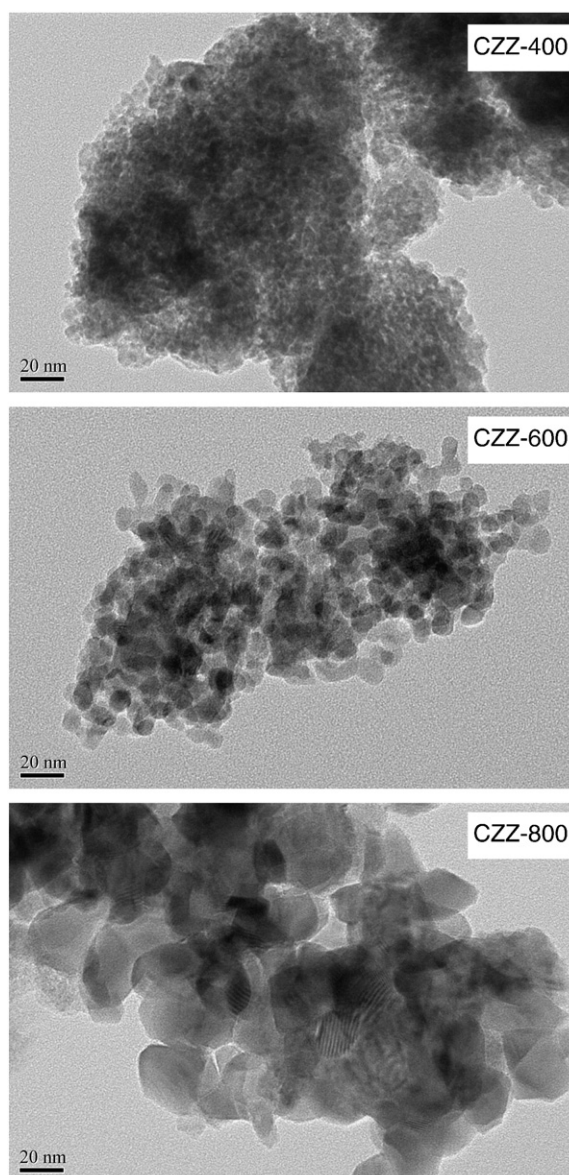


**Fig. 2.** TEM pictures of CZZ powders calcined at different temperatures.

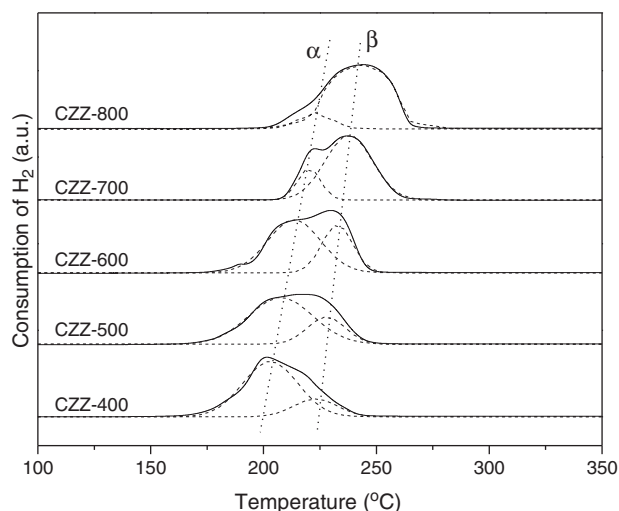


Fig. 3. H<sub>2</sub>-TPR profiles of the CZZ catalysts calcined at different temperatures.

performance of the resulting catalysts for methanol synthesis is shown in Table 1. It can be seen that the conversion of CO<sub>2</sub> decreases with the increase in calcination temperature. The variation trend can be explained in terms of the dispersion of Cu in CZZ catalysts. As well known, for copper-based catalysts, a higher dispersion of Cu usually results in a higher catalytic activity [18,21]. At the same time, the results of XRD and TPR measurements indicate that the dispersion of Cu decreases with the increase in calcination temperature. Consequently, a continued decline of catalytic activity from CZZ-400 to CZZ-800 is observed. Furthermore, it is noteworthy that a remarkable increase in methanol selectivity can be observed for CZZ-800 sample, although a very small difference is observed for the other samples (56.0–58.0%). The value of methanol selectivity over CZZ-800 is 63.3%, which is increased by about 13% relative to 56.2% of CZZ-700. This is because the methanol selectivity over *m*-ZrO<sub>2</sub>-supported catalysts is higher than that over *t*-ZrO<sub>2</sub>-supported catalysts [15,22], and zirconia in CZZ-800 sample exists mainly in monoclinic phase, as demonstrated by the XRD spectra.

The metallic copper surface area ( $S_{Cu}$ ) is an important parameter for Cu-based catalysts since metallic copper is extensively regarded as the main active component. As shown in Table 1, the methanol yield increases with the increase in the surface area of metallic copper, but it is not a linear relationship. This demonstrates that the activity of the CZZ catalyst is not only related to  $S_{Cu}$  but also to other causes. In this case, most probably, the synergy between metallic copper and the oxide components, which varies with the elevation of calcination temperature [18], is also responsible for the catalytic activity. Similar result was also reported by Sun et al. [23].

Under the same reaction conditions, the values of methanol yield are 7.7%, 8.5% and 9.6% over the CZZ catalysts with the same composition but prepared by carbonate co-precipitation, oxalate co-precipitation and urea-nitrate combustion methods, respectively [15]. Obviously, the catalyst prepared by the current method is more active than that derived from carbonate co-precipitation and oxalate co-precipitation methods, and it is comparable to the catalyst obtained by the urea-nitrate combustion method but with the merit of being solvent-free. Moreover, the most efficient sample CZZ-400 was selected for a stability measurement over a 96-h period. There is no visible decline in the CO<sub>2</sub> conversion and the methanol selectivity, indicating that the CZZ catalysts prepared via the route of solid-state reaction exhibit a stable catalytic performance for CO<sub>2</sub> hydrogenation.

Table 2

Temperature of reduction peaks and their contributions to the TPR pattern over the Cu/ZnO/ZrO<sub>2</sub> catalysts calcined at different temperatures.

Catalyst	T <sub>α</sub> (°C)	T <sub>β</sub> (°C)	A <sub>α</sub> /(A <sub>α</sub> + A <sub>β</sub> ) <sup>a</sup> (%)
CZZ-400	204	223	85.2
CZZ-500	208	228	74.5
CZZ-600	214	233	65.5
CZZ-700	220	238	19.3
CZZ-800	223	243	4.2

<sup>a</sup> A<sub>α</sub> and A<sub>β</sub> represent the area of α and β peak, respectively.

#### 4. Conclusions

Cu/ZnO/ZrO<sub>2</sub> catalysts were synthesized via a route of solid-state reaction between hydrated metal salts and citric acid ligand, which is found to be a simple, rapid and solvent-free method for the preparation of effective Cu/ZnO/ZrO<sub>2</sub> catalysts. The physicochemical properties and catalytic activity of the catalysts are strongly influenced by the calcination temperature. With the increase in calcination temperature, the dispersion of copper species decreases, and the phase transformation of zirconia from tetragonal to monoclinic occurs as the calcination temperature exceeds 600 °C. The CZZ catalyst calcined at 400 °C, which has the highest surface area of metallic Cu, exhibits an optimum catalytic activity.

#### Acknowledgments

The authors thank Science and Technology Commission of Shanghai Municipality (08520513600), Shanghai Municipal Education Commission (J51503) and Shanghai Institute of Technology (KJ2010-05) for financial support. The helpful suggestions provided by the anonymous reviewers are also gratefully acknowledged.

#### References

- [1] G.A. Olah, A. Goepfert, G.K.S. Prakash, *J. Org. Chem.* 74 (2009) 487–498.
- [2] F. Arena, K. Barbera, G. Italiano, G. Bonura, L. Spadaro, F. Frusteri, *J. Catal.* 249 (2007) 185–194.
- [3] Y.P. Zhang, J.H. Fei, Y.M. Yu, X.M. Zheng, *Energ. Conv. Manag.* 47 (2006) 3360–3367.
- [4] J. Słoczyński, R. Grabowski, A. Kozłowska, P. Olszewski, M. Lachowska, J. Skrzypek, *J. Stoch. Appl. Catal. A Gen.* 249 (2003) 129–138.
- [5] R. Raudaskoski, M.V. Niemelä, R.L. Keiski, *Top. Catal.* 45 (2007) 57–60.
- [6] Y. Ma, Q. Sun, D. Wu, W.H. Fan, Y.L. Zhang, J.F. Deng, *Appl. Catal. A Gen.* 171 (1998) 45–55.
- [7] J. Słoczyński, R. Grabowski, A. Kozłowska, P. Olszewski, J. Stoch, J. Skrzypek, M. Lachowska, *Appl. Catal. A Gen.* 278 (2004) 11–23.
- [8] Y. Nitta, T. Fujimatsu, Y. Okamoto, T. Imanaka, *Catal. Lett.* 17 (1993) 157–165.
- [9] P.F. Zhu, J. Li, S.F. Zuo, R.X. Zhou, *Appl. Surf. Sci.* 255 (2008) 2903–2909.
- [10] R.A. Köppel, C. Stöcker, A. Baiker, *J. Catal.* 179 (1998) 515–527.
- [11] C.L. Carnes, K.J. Klabunde, *J. Mol. Catal. A Chem.* 194 (2003) 227–236.
- [12] J. Agrell, M. Boutonnet, I. Melian-Cabrera, J.L.G. Fierro, *Appl. Catal. A Gen.* 253 (2003) 201–211.
- [13] L.C. Wang, Y.M. Liu, M. Chen, Y. Cao, H.Y. He, G.S. Wu, W.L. Dai, K.N. Fan, *J. Catal.* 246 (2007) 193–204.
- [14] X.M. Guo, D.S. Mao, G.Z. Lu, S. Wang, G.S. Wu, *J. Catal.* 271 (2010) 178–185.
- [15] X.M. Guo, D.S. Mao, S. Wang, G.S. Wu, G.Z. Lu, *Catal. Commun.* 10 (2009) 1661–1664.
- [16] T.N. Chen, B. Liang, X.Q. Xin, *J. Solid State Chem.* 132 (1997) 291–293.
- [17] X.R. Ye, D.Z. Jia, J.Q. Yu, X.Q. Xin, Z.L. Xue, *Adv. Mater.* 11 (1999) 941–942.
- [18] L.C. Wang, Q. Liu, M. Chen, Y.M. Liu, Y. Cao, H.Y. He, K.N. Fan, *J. Phys. Chem. C* 111 (2007) 16549–16557.
- [19] I. Melián-Cabrera, M. López Granados, J.L.G. Fierro, *J. Catal.* 210 (2002) 273–284.
- [20] N.F.P. Ribeiro, M.M.V.M. Souza, M. Schmal, *J. Power Sources* 179 (2008) 329–334.
- [21] G. Avgouropoulos, T. Ioannides, H. Matralis, *Appl. Catal. B Environ.* 56 (2005) 87–93.
- [22] M.D. Rhodes, A.T. Bell, *J. Catal.* 233 (2005) 198–209.
- [23] Q. Sun, Y.L. Zhang, H.Y. Chen, J.F. Deng, D. Wu, S.Y. Chen, *J. Catal.* 167 (1997) 92–105.